

The three dynamical fates of Boson Stars

F.S. Guzmán

*Instituto de Física y Matemáticas, Universidad Michoacana de San Nicolás de Hidalgo,
Edificio C-3, Cd. Universitaria, 58040 Morelia, Michoacán, México.*

Recibido el 26 de mayo de 2009; aceptado el 30 de junio de 2009

In this manuscript the three types of late-time behavior of spherically symmetric Boson Stars are presented, namely: stable configurations, unstable bounded that collapse and form black holes and unstable unbounded that explode. These three possibilities have been predicted by perturbation theory and other analytical results, whereas the full non-linear evolution of Boson Star configurations has verified the stable and unstable bounded cases using numerical relativity. In this paper also the unbounded case is confirmed to happen. In order to do so, Boson Star solutions are used as initial data of the Einstein-Klein-Gordon system of equations formulated as a constrained initial value problem, which in turn is solved using the finite differences approximation.

Keywords: Boson systems; numerical relativity; self-gravitating systems.

En este trabajo se presentan los tres tipos de comportamiento temporal de estrellas de bosones esféricamente simétricas, es decir: configuraciones estables, inestables que colapsan para formar agujeros negros e inestables que explotan. Estas tres posibilidades han sido predichas por la teoría de perturbaciones y otros resultados analíticos, mientras que la evolución no-lineal de las configuraciones de estrellas de bosones ha verificado los casos estable e inestable acotado usando relatividad numérica. En este artículo se confirma además el caso inestable no acotado. Para tal efecto, las soluciones de estrellas de bosones se usan como datos iniciales del sistema de ecuaciones de Einstein-Klein-Gordon formulado como un problema de valores iniciales con evolución restringida que resolvemos usando la aproximación con diferencias finitas.

Descriptores: Sistemas bosónicos; relatividad numérica; sistemas autogravitantes.

PACS: 05.30.Jp; 04.25.D-; 04.40.-b

1. Introduction

Boson Stars (BSs) are self-gravitating systems that help illustrate how more complicated systems -like neutron stars- evolve. Nevertheless, BSs have been studied not only as toy models but have also been considered as potentially existing astrophysical objects. In this sense, BSs can be assumed to potentially exist because they can be considered to represent the final stage of zero temperature self-gravitating Bose Condensates [1], with regular geometry and smooth matter distribution, with no horizons or singularities. Because these objects do not emit in the electromagnetic spectrum and do not interact in any way except through gravity, they are transparent. In fact BSs are studied as potential black hole candidates, with results that discard their existence such as those presented in [2], others showing that there must be significant differences when the model considers an accretion disk [3], and a third position showing that by choosing the correct Boson Star, that star can mimic the behavior of a black hole [4]. In a different context, the Newtonian version of BSs has been considered as a model of galactic halos, explaining the galaxy formation process under the scalar field dark matter hypothesis [1, 5–7]. For reviews on BSs see Refs. 8 and 9.

The relevance of the association of BSs with astrophysical objects becomes important when possible astrophysical measurable signals related to these objects might be at hand soon. This is the case of gravitational wave (GW) astronomy. There are already some results related to the GW signals sourced by Boson Stars, either single stars perturbed with shells of particles [10] or binary Boson Star systems [11].

The key point is that as gravitational wave sources are analyzed numerically, the technology is also applicable to the study of BS systems.

BS solutions, as happens with other type of general relativistic self-gravitating configurations, define a stable and an unstable branch. Nevertheless, the BS unstable branch shows a rather strange property, that is, there are unstable configurations that collapse into black holes and others that disperse away, because the binding energy is allowed to be negative or positive. It calls attention to the fact that the later configurations have not been studied sufficiently, and here we present important properties of this type of configurations. The results presented in this paper are related to the confirmation in the full non-linear regime of the three behaviors using the integration of an initial value problem using numerical relativity with the finite differences approximation. This study was presented before for the bounded cases [12, 13]. The unbounded case is presented for the first time as the confirmation of the predictions made using perturbation theory and other approaches (see *e.g.* Refs. 14 and 15).

The paper is organized as follows: in Sec. 2 the usual algorithm to construct BS configurations is shown, in Sec. 3 the algorithm used here to evolve BSs is presented; in Sec. 4 the configurations for the different types of behavior are selected; in Sec. 5 basic tests are shown for stable configurations; in Secs. 6 and 7 the expected behavior of unstable bounded and unbounded configurations (respectively) is presented; finally in Sec. 8 a few comments are mentioned.

2. Boson Star configurations

BSs arise from the Lagrangian density of a complex scalar field minimally coupled to gravity, that is:

$$\mathcal{L} = -\frac{R}{\kappa_0} + g^{\mu\nu} \partial_\mu \phi^* \partial_\nu \phi + V(|\phi|^2), \quad (1)$$

where $\kappa_0 = 16\pi G$ in units where $c = \hbar = 1$, ϕ is the scalar field, the star stands for complex conjugate and V the potential of self-interaction of the field [8, 9]. Notice that this Lagrangian density is invariant under the global $U(1)$ group, and the associated conserved charge is the amount called number of particles (defined below). When the action is varied with respect to the metric, Einstein's equations arise, $G_{\mu\nu} = \kappa_0 T_{\mu\nu}$, where the resulting stress-energy tensor reads

$$T_{\mu\nu} = \frac{1}{2} [\partial_\mu \phi^* \partial_\nu \phi + \partial_\mu \phi \partial_\nu \phi^*] - \frac{1}{2} g_{\mu\nu} [\phi^{*\alpha} \phi_{,\alpha} + V(|\phi|^2)]. \quad (2)$$

Boson Stars are related to the potential

$$V = m^2 |\phi|^2 + \frac{\lambda}{2} |\phi|^4,$$

although the name Boson Star has been applied to solutions using other types of potentials (see *e.g.* Ref. 16). The quantity m is understood as the mass of a boson and λ is the coefficient of a two-body self-interaction mean field approximation. The Bianchi identity reduces to the Klein-Gordon equation

$$\left(\square - \frac{dV}{d|\phi|^2} \right) \phi = 0, \quad (3)$$

where

$$\square \phi = \frac{1}{\sqrt{-g}} \partial_\mu [\sqrt{-g} g^{\mu\nu} \partial_\nu \phi].$$

Boson Stars (BSs) are spherically symmetric solutions to the above set of equations under a particular condition: the scalar field has a harmonic time dependence $\phi(r, t) = \phi_0(r) e^{-i\omega t}$, where r is the radial spherical coordinate. This condition implies that the stress energy tensor in Eq. (2) is time-independent, which implies through Einstein's equations that the geometry is also time-independent. That is, there is a time-dependent scalar field oscillating upon a time-independent geometry whose source is the scalar field itself. It is possible to construct solutions for Boson Stars assuming that the metric can be written in normal coordinates as

$$ds^2 = -\alpha(r)^2 dt^2 + a(r)^2 dr^2 + r^2 d\Omega^2. \quad (4)$$

For these coordinates the Einstein-Klein-Gordon (EKG) system of equations reads:

$$\begin{aligned} \frac{\partial_r a}{a} &= \frac{1 - a^2}{2r} \\ &+ \frac{1}{4} \kappa_0 r \left[\omega^2 \phi_0^2 \frac{a^2}{\alpha^2} + (\partial_r \phi_0)^2 + a^2 \phi_0^2 (m^2 + \frac{1}{2} \lambda \phi_0^2) \right], \\ \frac{\partial_r \alpha}{\alpha} &= \frac{a^2 - 1}{r} + \frac{\partial_r a}{a} - \frac{1}{2} \kappa_0 r a^2 \phi_0^2 (m^2 + \frac{1}{2} \lambda \phi_0^2), \\ \partial_{rr} \phi_0 + \partial_r \phi_0 \left(\frac{2}{r} + \frac{\partial_r \alpha}{\alpha} - \frac{\partial_r a}{a} \right) &+ \omega^2 \phi_0 \frac{a^2}{\alpha^2} \\ &- a^2 (m^2 + \lambda \phi_0^2) \phi_0 = 0. \end{aligned} \quad (5)$$

The system (5) is a set of coupled ordinary differential equations to be solved under the conditions of spatial flatness at the origin $a(0) = 1$, $\phi_0(0)$ finite and $\partial_r \phi_0(0) = 0$ in order to guarantee regularity and spatial flatness at the origin, and $\phi_0(\infty) = 0$ in order to ensure asymptotic flatness at infinity as described in Refs. 12 to 14, 17 and 18; these conditions reduce the system (5) to an eigenvalue problem for ω , that is, for every central value of ϕ_0 there is a unique ω with which the boundary conditions are satisfied. Because the system (5) presents several constants, it is convenient to re-scale the variables in such a way that they do not appear. In order to do so, the following transformation is convenient:

$$\begin{aligned} \tilde{\phi}_0 &= \sqrt{\frac{\kappa_0}{2}} \phi_0, \quad \tilde{r} = mr, \quad \tilde{t} = \omega t, \\ \tilde{\alpha} &= \frac{m}{\omega} \alpha \quad \text{and} \quad \Lambda = \frac{2\lambda}{\kappa_0 m^2}. \end{aligned}$$

The result is that the physical constants vanish from the equations and the radial coordinate has units of m and the time has units of ω . In fact the mass of the boson becomes the parameter that fixes the scale of the system. After substituting this transformation and removing the tildes from everywhere, the resulting EKG system of equations reads:

$$\begin{aligned} \frac{\partial_r a}{a} &= \frac{1 - a^2}{2r} \\ &+ \frac{1}{2} r \left[\phi_0^2 \frac{a^2}{\alpha^2} + (\partial_r \phi_0)^2 + a^2 (\phi_0^2 + \frac{1}{2} \Lambda \phi_0^4) \right], \\ \frac{\partial_r \alpha}{\alpha} &= \frac{a^2 - 1}{r} + \frac{\partial_r a}{a} - r a^2 \phi_0^2 (1 + \frac{1}{2} \Lambda \phi_0^2), \\ \partial_{rr} \phi_0 + \partial_r \phi_0 \left(\frac{2}{r} + \frac{\partial_r \alpha}{\alpha} - \frac{\partial_r a}{a} \right) &+ \phi_0 \frac{a^2}{\alpha^2} \\ &- a^2 (1 + \Lambda \phi_0^2) \phi_0 = 0. \end{aligned} \quad (6)$$

Notice that the bisected parameter ω now turns into the central value of the lapse α due to the rescaling. This is the system that is being solved in practice using finite differences with an ordinary integrator (adaptive step-size fourth-order Runge-Kutta algorithm in the present case) and a shooting routine that bisects the value of ω (the central value of α).

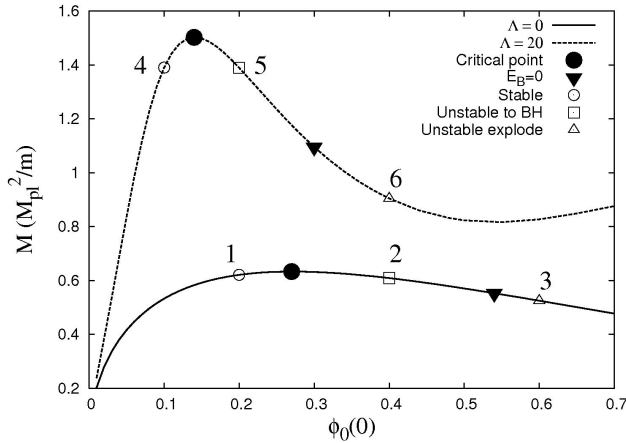


FIGURE 1. Sequences of equilibrium configurations for two values of Λ are shown as a function of the central value of the scalar field $\phi_0(0)$; each point in the curves corresponds to a solution of the eigenvalue problem and represents a Boson Star configuration. The filled circles indicate the critical solution that separates the stable from the unstable branch. Those configurations to the left of the maxima represent stable configurations. The inverted triangles indicate the point at which the binding energy is zero. Those configurations between the filled circles and the inverted triangles (along each sequence) collapse into black holes as a response to a perturbation. Configurations to the right of the inverted triangles disperse away.

The solutions to (6) define sequences of equilibrium configurations like those shown in Fig. 1. Each point in the curves corresponds to a Boson Star solution. In each of the curves two important points for each value of Λ are marked:

- i) the critical point -marked with a filled circle- indicating the threshold between the stable and unstable branches of each sequence, that is, configurations to the left of this point are stable and those to the right are unstable as found through the analysis of perturbations [14, 18], catastrophe theory [15] and full non-linear evolution of the equilibrium solutions [12, 13, 19] and
- ii) the point at which the binding energy $E_B = M - Nm = 0$ marked with an inverted filled triangle (see Ref. 14 for this convention of the binding energy), where

$$N = \int j^0 d^3x = \int \frac{i}{2} \sqrt{-g} g^{\mu\nu} [\phi^* \partial_\nu \phi - \phi \partial_\nu \phi^*] d^3x$$

is the number of particles; that is, the conserved quantity due to the invariance under the global $U(1)$ group of the Lagrangian density (1).

$M = (1 - 1/a^2)r/2$ evaluated at the outermost point of the numerical domain is the ADM mass; the configurations between the instability threshold and the zero binding energy point have negative binding energy ($E_B < 0$) and collapse into black holes, whereas those to the right have positive binding energy and disperse away. Last but most important, those configurations to the left of the threshold of instability, that is, stable configurations, obviously possess a negative

binding energy. The non-filled circles, triangles and squares pointed out in the plot correspond to the six configurations chosen as special cases to be developed here.

3. The evolution of Boson stars

As the main objective of this manuscript is to show the expected behavior of different sets of BS configuration, here we choose a simple way of dealing with the evolution process of the data constructed in the previous section. The strategy consists of splitting up the scalar field into its real and imaginary parts $\phi = \phi_1 + i\phi_2$. In this way, the Klein Gordon equation becomes two equations:

$$\left(\square - \frac{dV}{d|\phi|^2}\right)\phi_1 = 0, \quad \left(\square - \frac{dV}{d|\phi|^2}\right)\phi_2 = 0. \quad (7)$$

Another major point is that as time-dependence of the space-time is going to be allowed, the space-time metric has to be relaxed to:

$$ds^2 = -\alpha(r, t)^2 dt^2 + a(r, t)^2 dr^2 + r^2 d\Omega^2, \quad (8)$$

where time dependence of α and a has been set up, but the radial coordinate has been kept the same for simplicity. Using this new line element for the space-time, it is convenient to define first-order variables for the scalar field: $\pi_i = (a/\alpha)\partial_t\phi_i$ and $\psi_i = \partial_r\phi_i$, for each $i = 1, 2$. With these new variables and the metric (8), the KG equations are translated into the following set of PDEs of first order in space and time

$$\begin{aligned} \partial_t\phi_1 &= \frac{\alpha}{a}\pi_1, \\ \partial_t\phi_2 &= \frac{\alpha}{a}\pi_2, \\ \partial_t\psi_1 &= \partial_r\left(\frac{\alpha}{a}\pi_1\right), \\ \partial_t\psi_2 &= \partial_r\left(\frac{\alpha}{a}\pi_2\right), \\ \partial_t\pi_1 &= \frac{1}{r^2}\partial_r\left(r^2\frac{\alpha}{a}\psi_1\right) - a\alpha\frac{dV}{d|\phi|^2}\phi_1, \\ \partial_t\pi_2 &= \frac{1}{r^2}\partial_r\left(r^2\frac{\alpha}{a}\psi_2\right) - a\alpha\frac{dV}{d|\phi|^2}\phi_2. \end{aligned} \quad (9)$$

In terms of the first-order variables and the line element (8), Einstein's equations read:

$$\frac{\partial_r a}{a} = \frac{1 - a^2}{2r} + \frac{r}{2}[\pi_1^2 + \pi_2^2 + \psi_1^2 + \psi_2^2 + a^2V], \quad (10)$$

$$\frac{\partial_r \alpha}{\alpha} = \frac{a^2 - 1}{r} + \frac{a'}{a} - ra^2V, \quad (11)$$

$$\partial_t a = \alpha r[\psi_1\pi_1 + \psi_2\pi_2]. \quad (12)$$

These equations correspond to the Hamiltonian constraint, the slicing condition and the momentum constraint, respectively. Clearly, this set of equations is over-determined, and

TABLE I. Configurations used to present the three different types of behavior. The properties of the Gaussian shell acting as perturbation and the magnitude in percent of the perturbation are mentioned. The perturbation profile is $A \exp(-(r - r_0)^2/0.1)$. M is the mass of the unperturbed Boson Star, M_{pert} is the mass of the perturbed Star, % indicates the percent of mass the perturbation contributes with, r_{95} is the radius of the Star containing 95 per cent of the total mass of the star.

Label	M	M_{pert}	%	r_{95}	r_0	A
C1	0.620882		0.	7.66		
C2	0.608758	0.60937	0.1	4.84	6.	0.0008
C3	0.5248	0.52537	0.1086	3.68	5.	0.0012
C4	1.390156		0.	12.27		
C5	1.389544	1.39101	0.105	7.62	9.	0.0008
C6	0.9043	0.905234	0.103	5.66	7.	0.0008

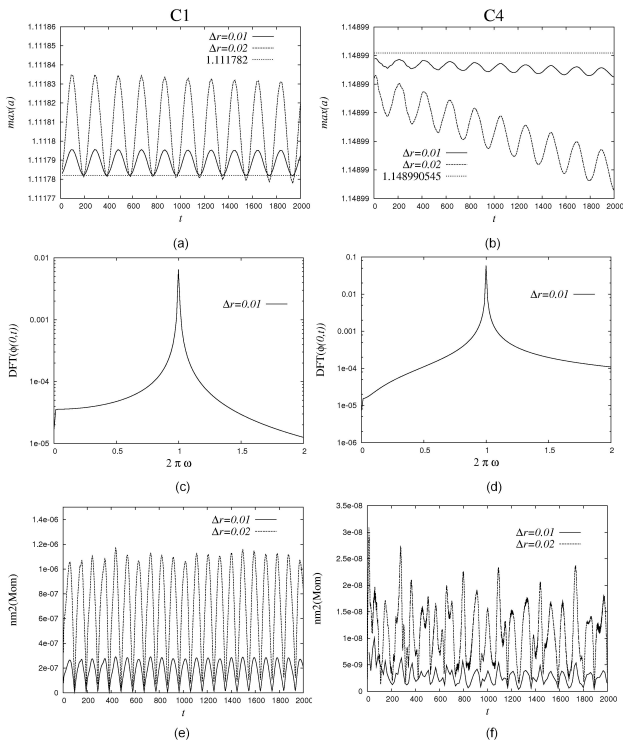


FIGURE 2. (top) Convergence of a_{max} for configurations 1 and 4. The constant line indicates the value of a_{max} at the initial time, which is assumed to be the value it should keep during the evolution. Second-order convergence to this value during evolution is a good indicator that the evolution is being carried out properly. (Middle) Fourier Transform of the central value of the field for the same configurations. The peak shows up at $\omega = 1/2\pi$. This test indicates that the scalar field is oscillating with the assumed frequency. (Bottom) Convergence of the 2-norm of the momentum constraint; the aim of these plots is to show that the momentum constraint (which was not considered to carry out the evolution of the system) is satisfied in the continuum limit. The numerical parameters are as indicated in the plots: two resolutions were used so that the convergence test was possible.

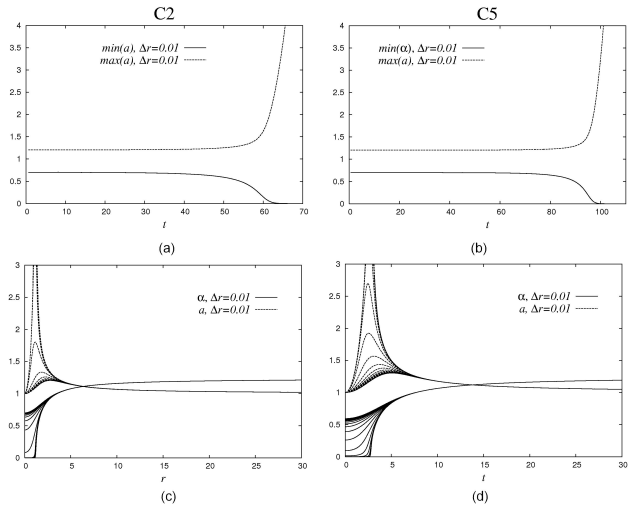


FIGURE 3. (Top) Maximum of the metric function a and minimum of α . What is shown is the collapse of the lapse and the divergence of a , which indicates the formation of a horizon in the coordinates that are being used. (Bottom) Snapshots of a and α that show the process of collapse. The resolution used is the one shown in the plots and the numerical domain is $r \in [0, 30]$ for the two configurations.

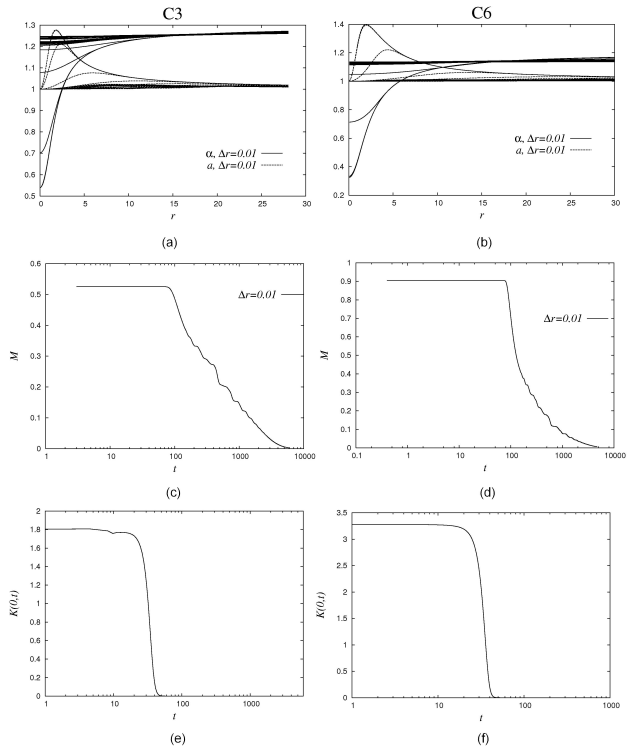


FIGURE 4. (Top) Snapshot of the metric functions for configurations C3 and C6. It is clear that the metric evolves toward the flat metric. (Middle) Mass vs time of the system, which shows that the configuration is releasing all its mass toward infinity. (Bottom) Central value of the Kretschmann scalar, which tends to zero with the pass of time. The resolution used is indicated in the plots.

it is necessary to choose two of these three equations as the set to be solved; the first two equations are solved and it is

verified that the momentum constraint is satisfied in the continuum limit using a Cauchy type of convergence test. Therefore the algorithm for the evolution consists in using (9) to evolve the system, then solve (10,11) and use the new values of the metric functions for the next step of the evolution.

The boundary condition for the scalar field is that of an outgoing spherical wave on a Schwarzschild background, which in its differential equation form reads:

$$\partial_r \pi_i + \partial_t \pi_i + \pi_i/r = 0, \quad \psi_i = -\pi_i - \phi_i/r, \quad (13)$$

for each $i = 1, 2$. That is, the real and imaginary parts of the scalar field are considered to behave as outgoing spherical waves separately. This is a quite simple boundary condition that certainly can be improved, the only requirement demanded in the present analysis being that the boundary conditions allow second-order convergence after various crossing times.

For the evolution of the scalar field variables we used a second-order accurate centered finite differences approximation, and the Method of Lines with a third order Runge-Kutta time integrator. Einstein's equations were integrated using a fourth-order Runge-Kutta ODE solver. The boundary conditions were implemented using a second-order approximation and an upwind stencil.

4. Preparing the states

In order to illustrate the three types of fate for Boson Stars, we choose three configurations for each of the two values of the self-interaction $\Lambda = 0, 20$, that clearly indicate the expected behavior. According to the labels in Fig. 1, the theory predicts that the results should be: configurations 1 and 4 should remain stable; configurations 2 and 5 should collapse to black holes; finally, configurations 3 and 6 should disperse away.

In Table I we summarize the properties of the configurations chosen. The selected stable configurations were not perturbed so that it was possible to track the convergence toward a time-independent geometry, whereas we used a gaussian shell to trigger the further evolution of the unstable configurations.

5. Stable configurations

The test consists in showing the validity of the hypotheses used in the construction of BS solutions (harmonic time dependence of the scalar field and time independence of the metric functions). The configurations proposed for the test are the configurations marked with unfilled circles and numbers 1 and 4 in Fig. 1.

In the top part of Fig. 1 the maximum of the metric function a is shown. Due to the discretization error, the configurations are perturbed permanently, and therefore the metric is oscillating in time. The point is that one has to show that the amplitude of the oscillations converges to zero, which is

equivalent to having the convergence of a_{max} to the value it should keep during all the evolution, which we consider to be the value of a_{max} calculated for the equilibrium configuration at the initial time. The oscillations of this metric functions were assumed to be a sort of quasi-normal mode oscillation, when first calculated for boson stars [13].

After the convergence toward a time-independent metric (achieved by monitoring the maximum of a), the main test of an evolution code consists in showing that the scalar field is truly oscillating meanwhile with the correct frequency. In the middle panel of Fig. 1 the Fourier Transform of the central value of ϕ_1 is shown. The result indicates that the frequency of oscillation of the scalar field corresponds to the eigenvalue calculated when solving the initial value problem (remember the time was rescaled to be $\tilde{t} = \omega t$). In the units used here, where $t \rightarrow \omega t$, the frequency is $\omega = 1/2\pi$.

For completeness, in the bottom panel of Fig. 1, second-order convergence of the momentum constraint is shown using two different resolutions. This indicates that in the continuum limit the momentum constraint is satisfied.

No explicit perturbations are applied in the stable case. Instead, measuring the correct frequency of oscillation of the scalar field determines whether or not the evolution code is working properly. Applying explicit perturbations to the particle number of these stable configurations would imply a more dynamical behavior, and the amplitude decay of the maximum of the metric function a as in Ref. 13.

6. Bounded unstable configurations

For this second case we choose the adequate configurations 2 and 5, which have a negative binding energy. In principle, the discretization error would provide a strong enough perturbation to collapse the configuration. However, in order to have a quicker collapse we use a small perturbation consisting of a Gaussian shell of particles implemented through the addition of a little Gaussian shell to the real part of the scalar field, with properties shown in Table I. Then the equations for α and a are resolved before starting the evolution. The amplitude of the Gaussian shell is positive and the number of particles (the Noether charge) is increased by a tiny fraction of the initial total charge (which reflects in the total mass of the perturbed configuration as well).

The results of the evolution are summarized in Fig. 3, where snapshots of the lapse and a are shown; in fact the lapse collapses to zero in a region expected to be covered by a horizon and the metric function a starts diverging due to the slice-stretching effect when using normal coordinates [20]. In the coordinates used, an apparent horizon, has been formed when the lapse is sufficiently near to zero. However, it is simple to use different coordinates allowing one to calculate the location, mass and possible oscillations of an apparent horizon. Up to this point the results in this section correspond to the typical results found for spherically symmetric BSs in the canonical papers [12, 13].

7. Unbounded unstable configurations

In this case, the binding energy is positive, which means that there is no work needed to disassemble the configuration. This is a case that is barely mentioned in BS research. As far as the author is aware, the potential first case of fissioned BS was shown in Ref. 19.

In Fig. 4 the results for configurations 3 and 6 are shown with three different arguments:

- i) the metric function a and the lapse α become constant after a while during the evolution,
- ii) the mass function M decays to zero during the same time-scale, and
- iii) the central value of the Kretschmann scalar K becomes zero, in order to have an indication that no singularities are left behind the exploding scalar field.

This is supported by the fact that the metric at the origin is spatially flat and with a non-zero lapse.

The perturbation consisted in the addition of a tiny fraction of particles again, even though the configurations reacted in a very explosive way.

The property assumed to be responsible for this explosive behavior is the one argued as that responsible for working against the gravitational collapse of the bosons, that is, the uncertainty principle, as opposed to the degeneracy pressure that prevents the gravitational collapse of fermionic stars. The implication of the uncertainty principle is therefore that the configuration has an excess of kinetic energy to compensate for the localization of the wave function.

8. Final remarks

Among the three types of Boson Stars presented here, only the stable type has been studied with certain attention, and stable configurations are proposed either as potential existing objects or as toy models. However, the unstable configurations might indicate restrictions on the properties of fundamental scalar fields (mass and self-interaction potential) that play different roles in cosmological models nowadays, from low energy limits of string theories to brane world models. Conversely, the properties of the scalar field might be restricted from fundamental theories and therefore the potential existence of BSs would be restricted also.

Acknowledgments

This work is partly supported by projects CIC-UMSNH-4.9, CONACyT 79995 and PROMEP-UMICH-CA-22.

A Kretschmann invariant

We use the central value of the Kretschmann invariant, in order to easily see the formation of a singularity. The expression for the metric (8) is:

$$\begin{aligned}
 K = & -\frac{16\dot{a}^2}{r^2\alpha^2a^4} + \frac{4(\alpha'')^2}{\alpha^2a^4} - \frac{8\alpha''\ddot{a}}{\alpha^3a^3} + \frac{8\alpha''\dot{\alpha}\dot{a}}{\alpha^4a^3} \\
 & - \frac{8\alpha''\alpha'a'}{\alpha^2a^5} + \frac{4(\ddot{a})^2}{\alpha^4a^2} - \frac{8\ddot{a}\dot{\alpha}\dot{a}}{\alpha^5a^2} + \frac{8\ddot{a}\alpha'a'}{\alpha^3a^4} \\
 & + \frac{4(\dot{\alpha})^2(\dot{a})^2}{\alpha^6a^2} - \frac{8\dot{\alpha}\dot{a}\alpha'a'}{\alpha^4a^4} + \frac{4(\alpha')^2(a')^2}{\alpha^2a^6} + \frac{8(\alpha')^2}{r^2\alpha^2a^4} \\
 & + \frac{8(a')^2}{r^2a^6} + \frac{4}{r^4} - \frac{8}{r^4a^2} + \frac{4}{r^4a^4}.
 \end{aligned}$$

-
1. F.S. Guzmán and L.A. Ureña-López, *ApJ* **645** (2006) 814; ArXiv: astro-ph/0603613.
 2. Y-F. Tuan, R. Narayan, and M.J. Rees, *ApJ* **606** (2004) 1112.
 3. D.F. Torres, *Nucl. Phys. B* **26** (2002) 377.
 4. F.S. Guzmán, *Phys. Rev. D* **73** (2006) 021501; ArXiv: gr-qc/0512081.
 5. A. Bernal and F.S. Guzmán, *Phys. Rev. D* **74** (2006) 063504; ArXiv: astro-ph/0608523.
 6. A. Bernal and F.S. Guzmán, *Phys. Rev. D* **74** (2006) 103002; ArXiv: astro-ph/0610682.
 7. E.W. Mielke and J.A. Vélez-Pérez, *Phys. Rev. D* **75** (2007) 043504; *Ibid, Phys.Lett. B* **671** (2009) 174.
 8. Ph. Jetzer, *Phys. Rep.* **220** (1992) 163.
 9. F.E. Schunck and E.W. Mielke, *Class. Quantum Grav.* **20** R301.
 10. J. Balakrishna, R. Bondarescu, G. Daues, F.S. Guzmán, and E. Seidel, *Class. Quantum Grav.* **23** (2006) 2631; ArXiv: gr-qc/0602078.
 11. C. Palenzuela, I. Olabarrieta, L. Lehner, and S. Liebling, *Phys. Rev. D* **75** (2007) 064005; ArXiv: gr-qc/0612067.
 12. E. Seidel and W-M. Suen, *Phys. Rev. D* **42** (1990) 384.
 13. J. Balakrishna, E. Seidel, and W-M. Suen, *Phys. Rev. D* **58** (1998) 104004.
 14. M. Gleiser, *Phys. Rev. D* **38** (1988) 2376.
 15. F.V. Kusmartsev *et al.*, *Phys. Rev. D* **43** (1991) 3895.
 16. F.E. Schunck and D.F. Torres, *Int. J. Mod. Phys. D* **9** (2000) 601.
 17. R. Ruffini and S. Bonazzolla, *Phys. Rev.* **187** (1969) 1767.
 18. S.H. Hawley and M.W. Choptuik, *Phys. Rev. D* **62** (2000) 104024.
 19. F.S. Guzmán, *Phys. Rev. D* **70** (2004) 044033.
 20. M. Alcubierre, *Introduction to 3+1 Numerical Relativity* (Oxford University Press, 2008).